

The effect of groundwater interaction in North American regional climate simulations with WRF/Noah-MP

Michael Barlage • Mukul Tewari • Fei Chen •
Gonzalo Miguez-Macho • Zong-Liang Yang •
Guo-Yue Niu

Received: 10 September 2013 / Accepted: 9 December 2014 / Published online: 24 February 2015
© Springer Science+Business Media Dordrecht 2014

Abstract The fluxes of water and energy between the land surface and atmosphere involve many complex non-linear processes. In this study, the Noah and Noah-MP land surface models with multiple groundwater sub-models are used to assess how the treatment of canopy processes and interactions with deep groundwater affect 6 month regional climate simulations in two contrasting years, 2002 and 2010. Unlike the free drainage models, the models with groundwater capability have upward flux from the aquifer at different periods in the simulation. The inter-model Noah-MP soil moisture and latent heat flux results are consistent with recharge differences: the stronger upward flux capability with interactive groundwater results in the highest soil moisture and latent heat flux of the Noah-MP models. The increased latent heat effect on increased precipitation is small, which may result from negligible differences in convective precipitation. The Noah-MP model, independent of groundwater option, improves upon a cold and dry bias in the spring Noah simulations both during the day and night. The results for summer are region dependent and also differ between year and time of day. For a majority of the simulation period, there is little groundwater effect on the Noah-MP near-surface diagnostic fields. However, when the Noah-MP model produces large warm/dry biases in the 2010 summer, the aquifer interactions in Noah-MP improve the air temperature bias by 1–2 °C and dew point temperature bias by 1 °C.

This article is part of a Special Issue on “Regional Earth System Modeling” edited by Zong-Liang Yang and Congbin Fu.

Electronic supplementary material The online version of this article (doi:10.1007/s10584-014-1308-8) contains supplementary material, which is available to authorized users.

M. Barlage (✉) • M. Tewari • F. Chen
National Center for Atmospheric Research, Boulder, CO, USA
e-mail: barlage@ucar.edu

G. Miguez-Macho
Universidade de Santiago de Compostela, Santiago, Spain

Z.-L. Yang
University of Texas, Austin, TX, USA

G.-Y. Niu
University of Arizona, Tucson, AZ, USA

1 Introduction

The land surface interacts with the atmosphere through interconnected water and energy fluxes at timescales that vary from seconds to years. Water stored in the land, as both soil moisture (SM) and deep groundwater (GW), is involved in processes that encompass the entire spectrum of these timescales. The effect of SM on atmospheric processes has been studied extensively in recent years, primarily through the feedback between SM and precipitation (P). These studies have involved how wet and dry regions affect surface energy partitioning, boundary layer characteristics, and thermally induced convection (e.g., Schar et al. 1999; Trier et al. 2008) with the potential of intensifying the hydrologic cycle (Dirmeyer et al. 2012; Zaitchik et al. 2013). SM differences and subsequent evaporation differences have been shown to increase P efficiency through increasing convective instability (Schar et al. 1999) and also to affect precipitation probability without affecting intensity (Findell et al. 2011). These studies generally examine climatological SM anomalies to determine how surface energy flux differences condition the convective boundary layer to inhibit or facilitate convective precipitation (Brimelow et al. 2011). The relationship between SM and P can depend on the reference state from which the anomaly is based, while the relationship with fluxes, and near-surface air temperature and moisture is not as dependent on the reference state (Barthlott and Kalthoff 2011).

Many studies have focused on the Central and Southern Great Plains in the United States due to observation- and model-based evidence of strong land surface coupling in this region (Koster et al. 2004; Zeng et al. 2010). Ferguson and Wood (2011) found that this region lies in a transition zone where the advantage for precipitation occurrence shifts from dry soil (Western US) to wet soil (Eastern US).

Land surface models (LSMs) have historically not considered the interactions of GW with SM in model-resolved soil layers. Using a coupled LSM-GW model with a prescribed atmosphere, Maxwell and Miller (2005) found only small differences in latent heat flux (LH) and sensible heat flux (SH), but large differences in runoff, primarily because shallow SM was similar with and without GW, but deep SM was not. With the same LSM-GW model, Kollet and Maxwell (2008) found a highly-sensitive water table depth (WTD) zone between 1 and 5 m, though the sensitivity to LH was dependent on vegetation type and transpiration formulation in the model. The surface energy partitioning and temperature sensitivity was highest in late summer, approaching 75 W/m² (LH) and 2 °C for deep versus shallow WTD, respectively (Ferguson and Maxwell 2010). Lateral GW transport has also been shown to be necessary to maintain wetter soil and higher LH in Amazon River valleys (Miguez-Macho and Fan 2012).

The length of LSM-GW simulations with an interactive atmosphere have generally been on the order of days (Seuffert et al. 2002; Maxwell et al. 2011) and show local LH feedbacks to atmospheric temperature. These studies also evaluate the magnitude of GW effects relative to specification of vegetation and soil type and find the GW effect to be of similar magnitude to vegetation for simulated LH and of greater magnitude for near-surface atmospheric temperature. Similar to the prescribed atmosphere simulations, LH shows a strong correlation to WTD and a GW component is necessary for the model to not dry out in shallow water table regions (Maxwell et al. 2007). Jiang et al. (2009) ran a coupled atmosphere-LSM-GW model for three summer months over the Central United States and found a 20 % increase in P, a 15 W/m² increase in average mid-day LH, and a 1 °C decrease in maximum surface temperature.

Therefore, the main objective of this study is to systematically examine effects of GW-surface-atmosphere interactions on seasonal prediction of surface weather and precipitation amount. This is accomplished using different GW interaction approaches of varying complexity and analyzing the feedbacks to an atmospheric model in 6-month regional climate model simulations over North America.

2 Methodology

2.1 Regional climate and land surface models

The Weather Research and Forecasting (WRF; Skamarock et al. 2008) model ARW version 3.4.1 is used as the regional climate model for this study. It is configured as a single grid domain with 30-km grid spacing (216 by 162 grid cells) spanning a majority of North America from about 15°N to 55°N (Fig. 1a). The following WRF model physics options are used for all simulations: Thompson microphysics scheme, CAM shortwave and longwave radiation scheme, Betts-Miller-Janjic cumulus scheme, and the YSU planetary boundary layer scheme. These physics options performed well in previous regional climate simulations over the western United States (Rasmussen et al. 2010).

Land surface processes are simulated using two available LSM options in WRF. The Noah land surface model (Chen and Dudhia 2001) is based on a Penman potential evaporation approach, a multi-layer soil model, and a primitive vegetation model. For groundwater interactions, Noah considers a free drainage lower boundary condition where the rate of water loss is based on hydraulic conductivity modulated by a slope factor (0.1 in WRF). Noah has no upward groundwater flow into the lowest soil layer, which is prescribed with a lower boundary at 2 m depth.

Another recently added WRF LSM option is the Noah-MP LSM (Niu et al. 2011). Noah-MP is unique among land surface models in that, like WRF, it has multiple options for key land-atmosphere interaction processes. Noah-MP was developed to improve upon some of the limitations of the Noah model. Noah-MP contains an explicit vegetation canopy defined by a canopy top, bottom and crown radius with two-stream radiation transfer in the canopy, and a multi-layer snow pack with liquid water storage. Multiple options are available for surface water infiltration and runoff, and groundwater transfer and storage within the four model soil layers that are defined the same as in Noah.

Within the Noah-MP model, three options for groundwater physics are used for this study. The first and least complex option (denoted MPR3 since it is option 3 within Noah-MP) is based on the free drainage approach of Noah with the same slope factor of 0.1. The second

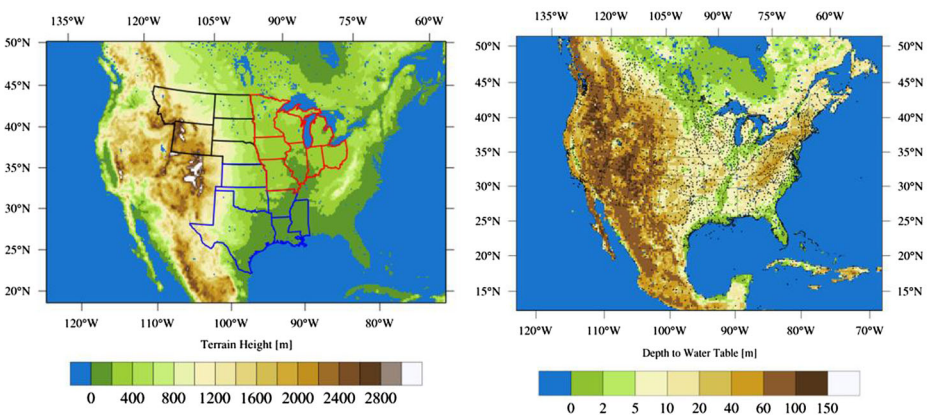


Fig. 1 Simulation domain and terrain height [m] (*left*) and equilibrium depth to water table [m] used to initialize MMF groundwater module (*right*). States outlined are grouped by color for analysis: Northern Plains (*black*), Upper Midwest (*red*) and South Central (*blue*). Dots indicate station observation locations for temperature and dewpoint analysis

option, denoted MPR1, is based on the unconfined aquifer approach of Niu et al. (2011). The temporal variation of water stored in the aquifer is determined by the residual of calculated recharge rate from the soil above minus the calculated discharge rate from the aquifer out of the grid. The third option (MPR5) is based on the water table dynamics model developed by Miguez-Macho et al. (2007; hereafter denoted MMF). The MPR5 approach is similar to MPR1 in that an aquifer is explicitly defined at a dynamically determined depth below or within the model soil layers. MPR5 also considers lateral flow of the aquifer water and groundwater-river exchange, though these processes are generally only important on higher resolution grids than are used in this study. An important difference between these two aquifer options is that when the aquifer is below the resolved soil layers (2 m), MPR5 adds additional soil layers between the resolved layers and the water table to more accurately calculate fluxes between the resolved layers and the aquifer. MPR5 also requires an input dataset of equilibrium water table depth defined through an offline process using 30 years of climatological recharge described in MMF (see Fig. 1b). For this study, the relatively shallow water table of the central United States is the focus.

In both the Noah and Noah-MP models, a soil water stress function defines how efficient transpiration will be in the model. To test model sensitivity, two stress functions are used in the Noah-MP simulations: one equivalent to the stress function in Noah (denoted B1) where transpiration ceases when SM drops below the wilting point and is unimpeded above a reference SM and another (denoted B2) that allows for more efficient transpiration relative to B1 for medium to high SM (lower reference SM) and less efficient transpiration for low SM (higher wilting point).

2.2 Simulation period

Model simulations are completed beginning 25 February and ending 31 August for 2 years, 2002 and 2010. The first week of the simulations are omitted from the analysis to allow the model atmosphere to spin-up. These 2 years are chosen for their anomalous climatic conditions within the United States determined from data obtained from the National Oceanic and Atmospheric Administration's National Climatic Data Center (NCDC). The March/April/May (MAM) temperature in 2002 was anomalously low in the north and high in the south, while the June/July/August (JJA) temperature was generally high across the country. Precipitation in 2002 was high in the east and low in the west for MAM, and low in the west and east and high in the north and southeast for JJA. Temperature in MAM 2010 was high in the northeast and low in the southwest, while for JJA it was high everywhere except for the extreme northwest. Precipitation in MAM 2010 had little clear pattern except for being slightly high in the northwest, but was high across the center of the country for JJA and low along the southern east and west coast. The simulations focus on the spring and summer when the most sensitivity to groundwater is expected.

Initial and lateral boundary conditions for the atmospheric model are taken from the North American Regional Reanalysis (NARR; Mesinger et al. 2006). Lateral boundary conditions are updated every three hours from NARR output. To achieve land surface state equilibrium prior to initialization and incorporate the preceding snow season, the LSMs are run for 1 year using the offline High Resolution Land Data Assimilation System (HRLDAS; Chen et al. 2007) and atmospheric forcing data from NARR. A 1-year spin-up allows the preceding snow season to influence the initial soil conditions.

2.3 Observations and regional consolidation

A regional approach is used to verify the model simulations. Three analysis regions (Fig. 1a) are defined based on the NCDC's nine climatically consistent regions within the United States. The north-central section of the country is split into two parts. The western five states are considered the Northern Plains (NP) and the eastern eight states are denoted the Upper Midwest (UM). The South Central (SC) region consists of the five states south of the two northern regions. These regions generally encompass the relatively shallow water table region in the central United States (Fig. 1b).

To evaluate the performance of Noah relative to Noah-MP and the performance of the different groundwater approaches within Noah-MP, observations of air temperature (T_{2m}), dew point temperature (T_d), and P are used. For P, a 0.25° daily gridded gauge-based precipitation data set (CPC 2013) is accumulated beginning March 1 of each year for the three regions and the entire United States. For T_{2m} and T_d , surface observations at four times daily (00 UTC, 06 UTC, 12 UTC, and 18 UTC) are obtained from the National Center for Environmental Prediction (NCEP) Global Surface Observational Weather Data archive of METAR and SYNOP stations (NCEP 2004). The number of observations available in 2002 (2010) are approximately 110 (125), 360 (435), 200 (330) and 1980 (2620) in NP region, UM region, SC region and the full domain, respectively. The observation locations are shown in Fig. 1b.

3 Results and discussions

Model simulation results and the subsequent analysis focuses on internal model processes and their impact on P, and near-surface T_{2m} and T_d . For brevity, figures are shown for only the 2010 simulations and differences between years are discussed in the text. Figures for 2002 are presented in the supplemental material.

3.1 Groundwater recharge

Recharge is defined here as the downward flux of water from the bottom boundary of the 2-m model soil column. In the Noah and MPR3 models, this water exits the modeling system as underground (as opposed to surface) runoff. In MPR1 and MPR5, recharge is either stored in the soil below the model soil column or in the aquifer. MPR1 and MPR5 also both allow for water to flow upward into the model soil levels from the aquifer. Figure 2 shows the accumulated recharge in 2010 for the three analysis regions and the entire domain. A negative slope indicates when water is moving into the model 2-m column from below. Note that the Noah and MPR1 models always have a positive slope.

Recharge for Noah and MPR3 generally have the same slowly rising pattern for the three regions with MPR3 having slightly more recharge in the summer for NP. MPR1 recharge shows a similar pattern among the three regions: little or no recharge in the first month, followed by upward transport into the soil column for the second month and then a steady downward flux for the final 4 months. For MPR5 in the NP region, recharge steadily increases in the first 4 months followed by a net zero flux for the region in the last 2 months. In UM and SC, the first 2 or 3 months have little recharge but there is a steady upward moisture transport for the final 3 months. In general, MPR1 has the largest recharge even with some upward flux in the first few months and MPR5 transports 10–20 mm of water

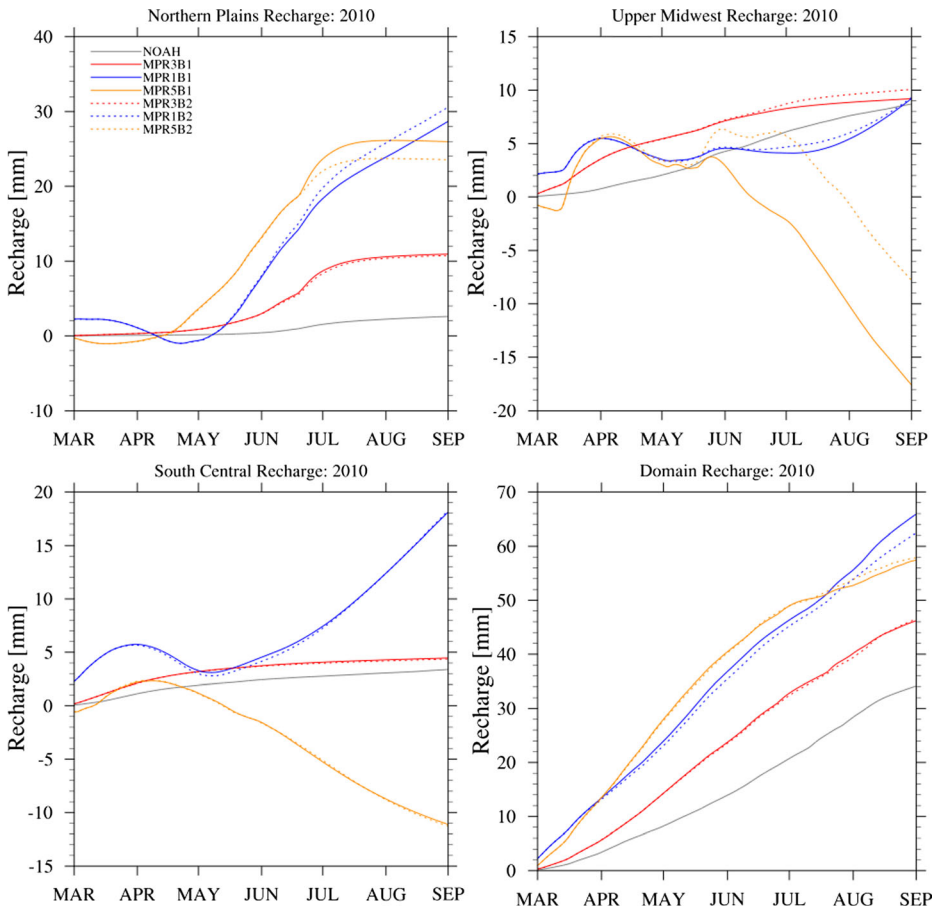


Fig. 2 Accumulated recharge [mm] defined as water flux out of the lower boundary of the 2-m soil column in the four models: Noah (grey), Noah-MP R3 (red), Noah-MP R1 (blue) and Noah-MP R5 (orange). Dashed lines are the Noah-MP options with the B2 soil moisture function. Negative slope implies upward transport. The panels are the three analysis regions and total domain (lower right)

upward from the aquifer in the summer months for the UM and SC regions. For the entire domain, Noah, MPR3 and MPR1 have steadily increasing recharge throughout the simulation resulting in 34, 46 and 66 mm of water loss after 6 months. MPR5 has the most recharge through July, but due to upward transport from the aquifer, levels off for the last 2 months ending with 58 mm.

The effect of water stress functions on runoff is mostly small except for MPR5 in the UM region, where in the final 3 months the B2 simulation has about 9 mm less upward transport. The recharge pattern for 2002 are similar, except that MPR1 does not have the upward flux in the second month and the magnitude of difference between Noah and MPR3 is larger. For MPR5 in 2002, the UM and SC regions still show upward transport in the final 3 months, but show a larger positive recharge at the beginning of the simulation compared to 2010 resulting in a net positive recharge in contrast to 2010. In 2002, the pattern for the total domain recharge is similar, but larger with 40, 85, 105, and 105 mm total recharge for Noah, MPR3, MPR1 and MPR5, respectively.

3.2 Soil moisture (SM)

The evolution of total column SM during the 6 months following the 1-year spin-up is shown in Fig. 3., illustrating the general features of soil recharge in spring and depletion in summer across regions. The relative difference between models remains consistent in the regions and the domain: Noah maintains the lowest SM (also indicated by the low spin-up value at initialization), MPR5 maintains the highest SM likely due to upward transport from the aquifer, and MPR3 and MPR1 are between with MPR1 generally lower due to more recharge (Fig. 2). The simulations show a SM increase in the NP region probably due to the above normal 2010 precipitation in this region. The other two regions and the full domain show little net flux in the first 3 months, followed by dry down over the final 3 months in all regions.

The effect of soil stress function on SM is small during the beginning of the simulation, but the B2 option increases SM at the end of the simulation in the drier UM and SC regions due to a reduced transpiration for low SM using the B2 option. For the entire domain, the B2 option decreases SM slightly because a larger portion of the domain is in the medium to high SM regime where B2 increases transpiration. In 2002, the relative pattern between Noah and Noah-

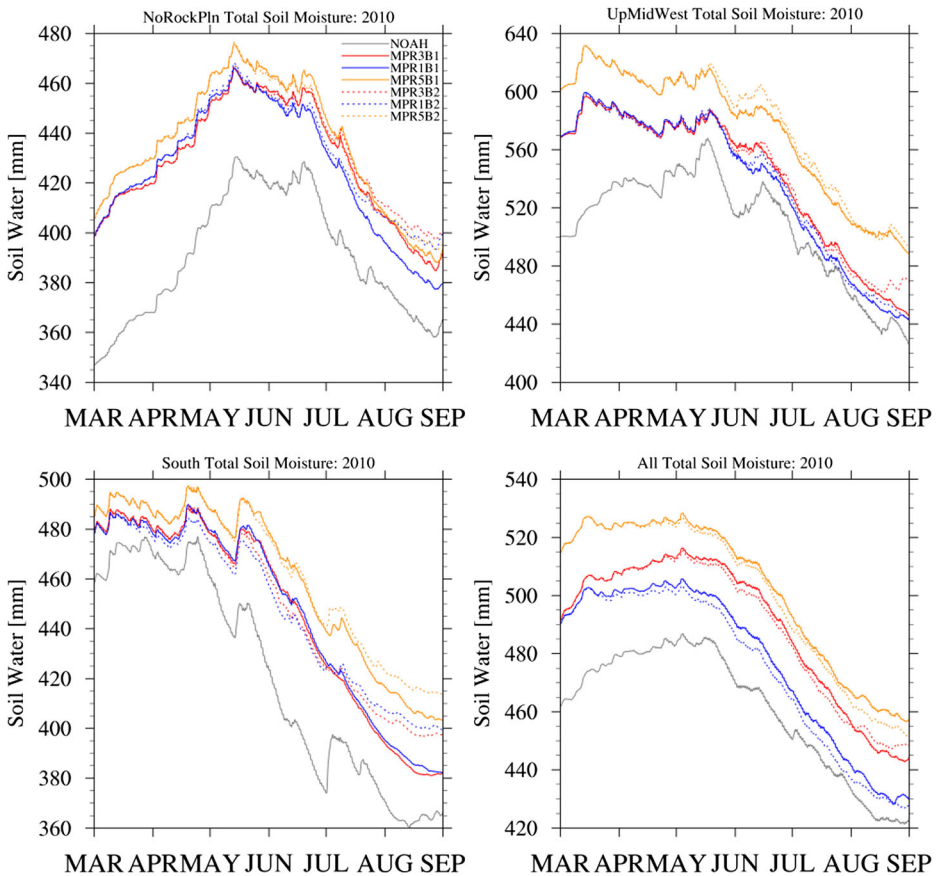


Fig. 3 Instantaneous total 2-m column soil moisture [mm] in the four models: Noah (grey), Noah-MP R3 (red), Noah-MP R1 (blue) and Noah-MP R5 (orange). Dashed lines are the Noah-MP options with the B2 soil moisture function. The panels are the three analysis regions and total domain (lower right)

MP is consistent with Noah being much drier. Differences among Noah-MP options, however, have a much smaller range than in 2010. This may be because the soil is generally wetter in 2002 resulting in greater recharge and less need for upward transport during the summer. The main separation between the MP options in 2002 occurs for the domain average where MPR1 is lower than the other two options.

3.3 Latent heat flux

The communication of inter-model SM differences to the atmosphere occurs through LH. Compared to the accumulated 6-month LH, the inter-model differences can be small (<20 %), so Fig. 4 shows the differences relative to the Noah model. The accumulated Noah LH in NP, UM, SC and total domain are 380, 560, 420 and 410 mm, respectively. Figure 4 shows that in 2010 by the end of the 6 months, all Noah-MP simulations have less LH than Noah. In the UM regions, the first 4 months of the simulation are higher than Noah, but are much less than Noah in the final 2 months. The difference between the Noah-MP options is consistent with SM.

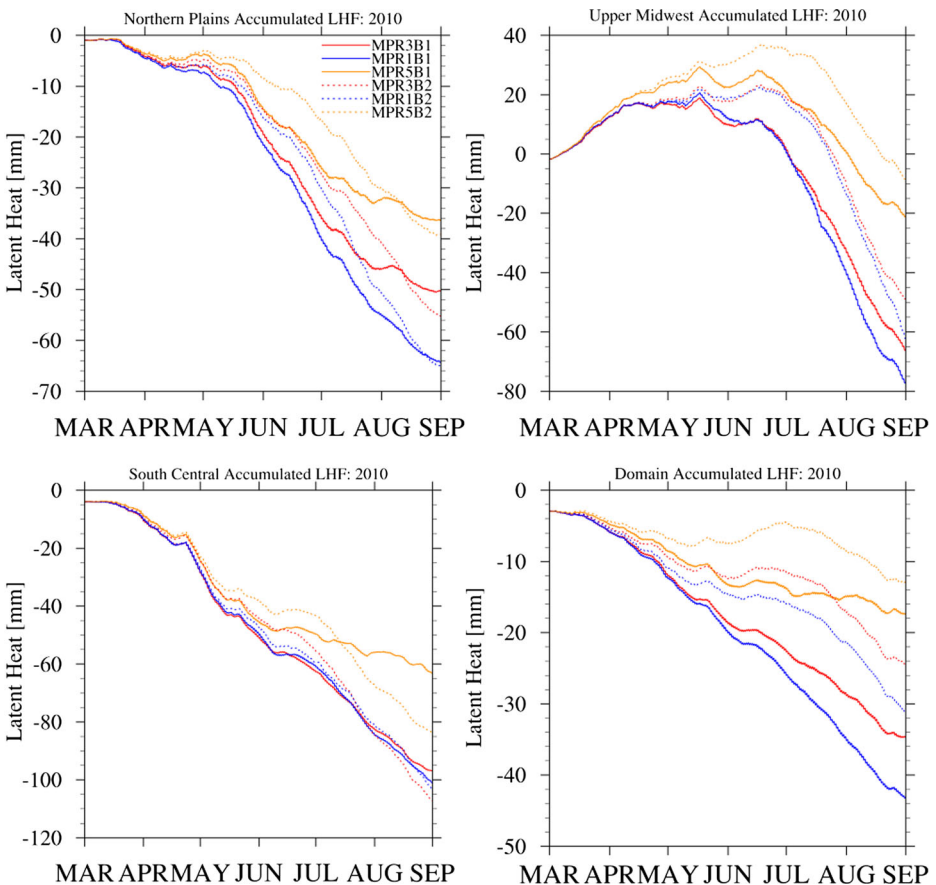


Fig. 4 Accumulated latent heat flux difference [mm] relative to the Noah model in the three Noah-MP models: R3 (red), R1 (blue) and R5 (orange). Dashed lines use the B2 soil moisture function. The panels are the three analysis regions and total domain (lower right)

MPR5 has the highest LH and MPR1 the lowest. The Noah-MP options tend to diverge in the final months of the simulation, consistent with the relative soil moisture in each simulation.

The effect of the soil stress functions on the Noah-MP simulations is also consistent with their effect on SM. The B2 option increases transpiration, and thus LH, in the early summer when SM is higher, but decreases LH due to less efficient transpiration when soils are drier as occurs in the later summer months. The net effect of these options is small in the NP and SC regions, but increases LH in the UM region and in the entire domain. In 2002, the differences relative to Noah are opposite. The LH relative to Noah in the NP and SC regions and full domain are higher by about 50, 30 and 25 mm, respectively. The UM region has a similar pattern to 2010 increasing to about 40 mm at the beginning of July, but the late summer decrease is small and the resulting difference from Noah at the end of the simulation is about zero. The 2002 inter-model Noah-MP differences are the same as in 2010 with MPR5 having the highest and MPR1 the lowest LH.

3.4 Precipitation (P)

The accumulated regional and domain precipitation compared to observed 2010 precipitation and to a 30-year precipitation climatology are shown in Fig. 5. Observed P in March–April–May (MAM) was generally close to the climatology in these three regions and the domain. June–July–August (JJA) P was normal in the SC region and above normal in NP, UM and in the domain. Simulated P is similar between models and with the observations for MAM. Noah starts to accumulate more P than Noah-MP by the end of the May, which is more consistent with observations. In JJA, the Noah simulations produce more P than Noah-MP but are still substantially lower than observations, especially in the SC region. The Noah-MP simulations produce about 25–50 % too little P in the three regions and 10–15 % too little for the domain. The difference relative to Noah is consistent with the lower LH, if P is assumed to result from local sources. The inter-model Noah-MP results are also consistent with the LH results. MPR5 generally produces more P than the other two GW options. The convective precipitation produced by the models is very similar (Fig. 5) implying that the main source of difference between the model simulations is in large-scale precipitation.

The effect of soil stress function is shown in Fig. 5 only for the MPR5 simulation. The B2 option has little effect on the P except in the UM region where the P decreased by about 8 % compared to the B1 option even though the LH increased with this option between June and July. Consistent with the relative differences in LH in 2002, the Noah-MP simulations produced more P than the Noah simulation, though the inter-model differences were smaller. The models all performed well in the UM region in 2002 where P was near normal. In the NP and SC regions, where P was below normal, the models produced too much P in NP and too little in SC. For the entire domain, the models produced about 10 % too much P.

Since P provides the flux of water into the top of the soil column and is a source for eventual LH, the net flux at the soil column top (P minus LH) is important for diagnosing model processes. As mentioned above, the 2010 Noah-MP simulations produce less P (Fig. 5) and less LH (Fig. 4) than when using Noah. For MPR3 relative to Noah, the decrease in LH is nearly the same as the decrease in P (50 mm, 65 mm, and 100 mm in regions NP, UM, and SC). For MPR1 relative to Noah, the decrease in LH is lower than that in P especially in the UM region where the accumulated P decrease is about 55 mm higher than the latent heat decrease. This implies that without significant flux of water from below, which is not seen in the summer months in MPR1, the soil column dries through the simulation (Fig. 3). The opposite effect is seen with MPR5, where P decreases of 50, 60 and 70 mm for the NP, UM and SC regions result in LH decreases of 35, 20 and 60 mm. The MPR5 simulation is able to

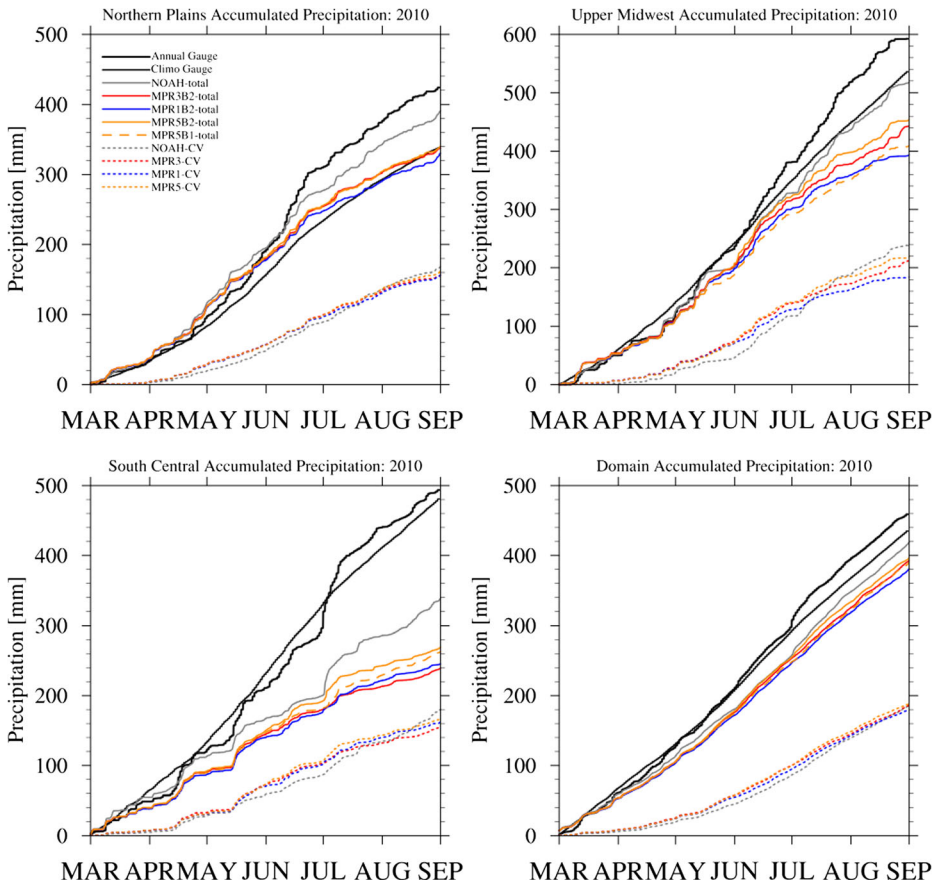


Fig. 5 Accumulated total precipitation [mm] in the four models: Noah (grey), Noah-MP R3 (red), Noah-MP R1 (blue) and Noah-MP R5 (orange). The long dashed orange line is the Noah-MP options with the B2 soil moisture function. Dashed lines (CV) are the convective component of the precipitation. Black lines are from NCDC gauge precipitation from 2010 (thick black) and 1971–2000 climatology. The panels are the three analysis regions and total domain (lower right)

maintain higher SM and LH due to upward flux of moisture from below (Fig. 2). A similar effect can be seen in 2002 for MPR5 where P differences relative to Noah of 25, 0 and 40 mm produce increases of LH of 60, 17 and 52 mm for regions NP, UM and SC, respectively.

3.5 Surface air temperature and moisture

The WRF model output contains 2-m air temperature and water vapor mixing ratio, which are diagnosed from surface temperature/moisture (Noah) or canopy air temperature/vapor pressure (Noah-MP) and surface sensible heat and LH. Therefore, altered surface energy budget terms, like those shown with LH (Fig. 3), will affect these surface diagnostics. To assess the performance of Noah and the several Noah-MP options, comparisons are done with surface observations of T_{2m} and T_d at about 2000 METAR and SYNOP sites (NCEP 2004) in the domain. The model results are adjusted to the elevation of the station data using a lapse rate of 6.5 °C/km. The observations are split into seasonal (MAM and JJA), and day (00/18 UTC) and night (06/12 UTC).

Model T_{2m} bias and root mean square error (RMSE) in 2002 and 2010 for the three regions (NP, UM, and SC) and full domain (ALL) are shown in Table 1 for all seasons and times of day. In MAM, both in 2002 and 2010, the Noah model shows a consistent cold bias of between 1.5 and 4.0 °C for all regions and the entire domain. This bias is present both during the day and night, and is usually larger during the day. Using any of the Noah-MP options reduces this bias by about 1.5 to 2.0 °C in the NP and SC regions in 2002 and improves the RMSE by 0.5 to 2.0 °C. The bias reduction is between 2.0 and 2.5 °C for the UM region and the entire domain. In 2010, Noah-MP overcorrects the cold bias in the NP region and results in a warm bias of about 2.0 °C (day) and 1.5 °C (night), though the RMSE is still similar to Noah. Even though the overcorrection is too large in the UM and SC regions, the magnitude of the warm bias is still smaller than the Noah cold bias. For the entire domain, the Noah-MP results show a large improvement in both bias and RMSE.

In JJA, daytime 2002 T_{2m} bias and RMSE are not significantly different between the four simulations in the three regions. Noah-MP bias and RMSE are larger in the UM regions, which may result from decreased LH relative to Noah in the last 2 months of the simulation. Nighttime JJA Noah T_{2m} bias ranges from 0.5 °C in the NP region to -0.6 and -1.2 °C in SC and UM, respectively. The Noah-MP simulations increase the nighttime T_{2m} by about 1.0 to 1.5 °C, mostly independent of groundwater option, thereby improving the simulations in UM and SC, but degrading them in NP. For the full domain, Noah has a cold bias of 0.5 °C (day) and 1.5 °C (night). The daytime bias for Noah-MP is near zero and the nighttime cold bias is about 0.5 °C using any groundwater option. The daytime RMSE between the models is similar, but the Noah nighttime RMSE was reduced about 0.7 °C by using Noah-MP.

For 2010, Noah has a 1.0 to 1.8 °C warm bias in the regions and a zero bias over the full domain during the day. In contrast to 2002, the Noah-MP daytime T_{2m} are significantly higher

Table 1 Seasonal 2-m air temperature bias and RMSE for each region and the whole domain. Noah-MP results use the B2 soil stress option

		MAM	MAM	JJA	JJA	MAM	MAM	JJA	JJA
		Day	Night	Day	Night	Day	Night	Day	Night
		2002	2002	2002	2002	2010	2010	2010	2010
NP	Noah	-1.8 (2.9)	-1.2 (2.1)	1.2 (2.6)	0.4 (1.7)	-1.5 (2.8)	-0.8 (1.8)	1.0 (2.1)	0.0 (1.7)
	MPR3	0.3 (2.0)	0.4 (2.0)	1.0 (2.3)	1.4 (2.2)	2.3 (3.0)	1.5 (2.2)	3.0 (3.5)	2.4 (2.8)
	MPR1	0.3 (2.0)	0.4 (2.0)	0.6 (2.4)	1.2 (2.3)	2.4 (3.1)	1.6 (2.2)	3.7 (4.1)	3.0 (3.3)
	MPR5	0.3 (2.0)	0.3 (1.9)	1.1 (2.2)	1.4 (2.1)	2.2 (2.9)	1.4 (2.1)	2.4 (3.1)	2.0 (2.5)
UM	Noah	-4.0 (5.0)	-3.7 (4.5)	1.1 (2.4)	-1.2 (2.4)	-2.7 (4.4)	-1.8 (2.9)	1.8 (2.7)	-0.3 (2.2)
	MPR3	-1.3 (3.0)	-1.6 (3.4)	1.7 (3.2)	0.3 (2.4)	1.8 (2.8)	1.3 (2.3)	4.2 (4.9)	2.0 (3.1)
	MPR1	-1.1 (3.0)	-1.6 (3.4)	1.9 (3.6)	0.4 (2.6)	1.9 (2.7)	1.3 (2.2)	5.1 (5.6)	2.6 (3.6)
	MPR5	-1.1 (3.0)	-1.6 (3.4)	1.8 (3.0)	0.2 (1.9)	1.6 (2.6)	1.1 (2.2)	3.0 (4.0)	1.0 (2.6)
SC	Noah	-1.4 (2.8)	-2.0 (2.8)	2.2 (3.0)	-0.6 (1.4)	-2.1 (3.2)	-2.3 (2.9)	1.8 (2.8)	-1.0 (1.6)
	MPR3	0.5 (2.3)	-0.3 (2.0)	2.4 (3.3)	0.4 (1.9)	1.9 (2.9)	1.1 (2.1)	4.2 (4.8)	1.6 (2.2)
	MPR1	0.6 (2.4)	-0.2 (2.0)	1.7 (2.7)	0.1 (1.9)	2.0 (2.9)	1.1 (2.1)	4.7 (5.4)	1.9 (2.7)
	MPR5	0.4 (2.2)	-0.1 (1.9)	2.3 (3.0)	0.4 (1.4)	1.7 (2.7)	1.0 (2.1)	3.7 (4.4)	1.3 (2.1)
ALL	Noah	-3.6 (3.9)	-3.1 (3.4)	-0.6 (1.0)	-1.5 (1.7)	-2.8 (3.2)	-2.0 (2.2)	-0.0 (0.8)	-1.0 (1.4)
	MPR3	-1.2 (1.7)	-0.8 (1.7)	0.1 (1.1)	-0.4 (1.0)	0.5 (1.0)	0.2 (0.8)	1.7 (1.9)	0.5 (1.0)
	MPR1	-1.1 (1.7)	-0.7 (1.8)	0.1 (1.2)	-0.5 (1.1)	0.5 (1.1)	0.2 (0.8)	2.1 (2.3)	0.8 (1.2)
	MPR5	-1.1 (1.7)	-0.9 (1.9)	0.2 (0.9)	-0.5 (0.9)	0.4 (1.0)	0.2 (0.8)	1.1 (1.6)	0.1 (0.9)

by about 1.5 to 3.3 °C in the regions and 1.0 to 2.0 °C over the whole domain. This may result from the drier soils and lower LH present in the model that year (see Sec. 3.2 and 3.3). RMSE is also higher by 1.0 to 2.0 °C for daytime JJA T_{2m} . At night in 2010, Noah has between a zero bias (NP) and 1.0 °C cold bias (SC) during JJA. Similar to the daytime, Noah-MP is warmer by about 1.0 to 3.0 °C at night with RMSE increases of 0.5 to 1.5 °C. Over the whole domain, Noah-MP performs better than Noah improving the 1.0 °C cold bias to about a 0.5 °C warm bias and reducing the RMSE slightly.

Compared to 2002 where there was little effect from the groundwater options, the warmer and drier simulation in 2010 is allowing the different groundwater options to have an effect on the simulations. The MPR5 simulations had a wetter soil, produced more LH and had upward transport of aquifer soil water in JJA relative to the other Noah-MP simulations. The MPR1 simulation had the driest soil, least LH, and largest discharge. These relative differences are consistent with 2010 JJA daytime and nighttime T_{2m} . In the NP and SC regions and the whole domain, the MPR5 simulations are about 0.5 °C cooler than the MPR3 simulations and about 1.0 °C cooler than the MPR1 simulations. In the UM region, the effect is about double with MPR5 being about 2.0 °C cooler than MPR1. At night, the results are similar with MPR5 producing the lowest warm bias and almost zero bias for the whole domain. The Noah-MP RMSE results are consistent with the warm bias reduction.

Model dew point temperature (T_d) bias and root mean square error (RMSE) in 2002 and 2010 for the three regions and full domain are discussed below and shown in a supplemental table for all seasons and times of day. In MAM, both in 2002 and 2010, the Noah model shows a consistent dry bias of between 1.0 and 2.5 °C for all regions and the entire domain. This bias is present both during the day and night, and is usually larger during the night. Using any of the Noah-MP options reduces the daytime T_d bias to less than 0.5 °C and the nighttime bias to less than 1.0 °C in 2002. In 2010, the regional performance of Noah-MP relative to Noah is mixed. Noah-MP overcorrects the Noah dry bias and is too moist in the UM region, but performs better than Noah both during the day and night for the SC region. In the NP region, Noah-MP makes the dry bias worse during the day, but improves the dry bias at night. For the entire domain, the Noah-MP results show a large improvement in both T_d bias and RMSE in both years. There are no significant differences between the Noah-MP groundwater options in MAM.

In JJA, T_d bias and RMSE in 2002 have regionally dependent improvement and degradation when comparing Noah and Noah-MP. In the NP region, Noah-MP shows a dry bias both during the day and night, but improves the Noah dry bias by about 2.0 °C and RMSE by 1.0 to 1.5 °C. In the UM region, the daytime dry bias is 1.0 to 2.0 °C higher in Noah-MP, but the nighttime bias is similar or slightly better than Noah. Depending on the groundwater option used, the results in the SC region are either the same (MPR3) as Noah or up to 1.0 °C improved (MPR1). For the entire domain, daytime T_d bias and RMSE are the same in the Noah and Noah-MP simulations, but nighttime T_d bias and RMSE are about 1.0 °C improved when using Noah-MP.

For 2010, the pattern of T_d difference between Noah and Noah-MP are similar. In the NP region, Noah-MP performs better than Noah, especially at night. In the UM and SC regions, Noah-MP performs worse than Noah during the day, but has a similar performance at night. This pattern can also be seen over the entire domain in 2010, where Noah-MP increases the dry bias during the day by about 0.5 °C and improves the dry bias by a similar magnitude at night.

There is not a clear universal effect of groundwater option on the Noah-MP T_d results. In both 2002 and 2010, the MPR1 and MPR5 simulations perform marginally better than MPR3 in the regional analysis, but do not improve the full domain results significantly. Similar to the

T_{2m} results above, when Noah-MP has a large dry bias (e.g., JJA in 2010 day and night), the MPR5 results have the lowest bias and RMSE and reduce the dry bias from the other options by 0.5 to 1.0 °C.

4 Conclusions

The fluxes of water and energy between the land surface and atmosphere involve many complex non-linear processes. In this study, two different LSMs, one with multiple GW options, are used to assess how the treatment of canopy processes and interactions with deep GW affect seasonal regional climate simulations. In contrast to the free drainage models, the models that have GW modeling capability do have upward flux from the aquifer at different periods in the simulation. The Noah SM is always lower than in Noah-MP, which is likely due to model climatology differences. The inter-model Noah-MP SM and LH results are consistent with recharge differences: the stronger upward flux capability of MPR5 results in the highest SM and LH of the Noah-MP models similar to previous studies (e.g., Maxwell et al. 2007). The effect of GW interaction is particularly evident when analyzing net water flux ($P - LH$) at the soil surface. The two simulation years have different LH results relative to Noah, but are consistent among Noah-MP options. In contrast to Jiang et al. (2009), the increased LH effect on increased P is small. This may be a result of the negligible difference in convective precipitation, potentially decreasing local recycling. However, the LH-P relationship (increased LH, increased P) is consistent among the regions and the domain.

The Noah-MP model, independent of GW option, in general improves upon a cold and dry bias in the spring (MAM) Noah simulations both during the day and night. The T_{2m} and T_d results for summer (JJA) are region dependent and also differ between night and day. For a majority of the simulation period, there is little GW effect on the Noah-MP near-surface diagnostic fields. However, when the Noah-MP model produces large warm/dry biases in the 2010 summer, the aquifer interactions of the MPR5 model alleviates the T_{2m} bias by 1–2 °C.

Acknowledgments Research support was provided through grants from the Joint Center for Satellite Data Assimilation (Grant no. NA13NES4400003) and National Oceanic and Atmospheric Administration (MAPP-CTB grant no. NA14OAR4310186).

References

- Barthlott C, Kalthoff N (2011) A numerical sensitivity study on the impact of soil moisture on convection-related parameters and convective precipitation over complex terrain. *J Atmo Sci* 68:2971–2987
- Brimelow J, Hanesiak J, Burrows W (2011) Impacts of land – atmosphere feedbacks on deep, moist convection on the Canadian prairies. *Earth Interact* 15:1–29
- Chen F, Dudhia J (2001) Coupling an advanced land surface-hydrology model with the Penn State-NCAR MM5 modeling system. Part I: model implementation and sensitivity. *Mon Weather Rev* 129:569–585
- Chen F et al (2007) Description and evaluation of the characteristics of the NCAR high-resolution land data assimilation system during IHOP-02. *J Appl Meteorol Climatol* 46:694–713
- CPC (2013) CPC US Unified Precipitation data provided by the NOAA/OAR/ESRL PSD, Boulder, Colorado, USA, from their Web site at <http://www.esrl.noaa.gov/psd/>
- Dirmeyer P et al (2012) Evidence for enhanced land-atmosphere feedback in a warming climate. *J Hydrometeor* 13:981–995
- Ferguson IM, Maxwell RM (2010) Role of groundwater in watershed response and land surface feedbacks under climate change. *Water Resour Res* 46, W00F02. doi:10.1029/2009WR008616

- Ferguson CR, Wood EF (2011) Observed land–atmosphere coupling from satellite remote sensing and reanalysis. *J Hydrometeorol* 12:1221–1254
- Findell K, Gentile P, Lintner B, Kerr C (2011) Probability of afternoon precipitation in eastern United States and Mexico enhanced by high evaporation. *Nat Geosci* 4:434–439
- Jiang X, Niu G-Y, Yang Z-L (2009) Impacts of vegetation and groundwater dynamics on warm season precipitation over the Central United States. *J Geophys Res* 114, D06109. doi:10.1029/2008JD010756
- Kollet SJ, Maxwell RM (2008) Capturing the influence of groundwater dynamics on land surface processes using an integrated, distributed watershed model. *Water Resour Res* 44, W02402. doi:10.1029/2007WR006004
- Koster RD et al (2004) Regions of strong coupling between soil moisture and precipitation. *Sci* 305:1138–1140
- Maxwell RM, Miller NL (2005) Development of a coupled land surface and groundwater model. *J Hydrometeorol* 6:233–247
- Maxwell RM et al (2007) Development of a coupled groundwater – atmosphere model. *Mon Weather Rev* 139: 96–116
- Maxwell RM, Chow FK, Kollet SJ (2011) The groundwater land- surface-atmosphere connection: soil moisture effects on the atmospheric boundary layer in fully-coupled simulations. *Adv Wat Resour* 30:2447–2466
- Mesinger, F., et al (2006) North American Regional Reanalysis. *Bull. Amer. Meteor. Soc.*, 87:343–360.
- Miguez-Macho G, Fan Y (2012) The role of groundwater in the Amazon water cycle: 2. Influence on seasonal soil moisture and evapotranspiration. *J Geophys Res* 117, D15114. doi:10.1029/2012JD017540
- Miguez-Macho G, Fan Y, Weaver CP, Walko R, Robock A (2007) Incorporating water table dynamics in climate modeling: 2. Formulation, validation, and soil moisture simulation. *J Geophys Res* 112, D13108. doi:10.1029/2006JD008112
- National Centers for Environmental Prediction (2004) NCEP ADP Global Surface Observational Weather Data, retrieved from <http://rda.ucar.edu/datasets/ds461.0/>
- Niu G-Y et al (2011) The community Noah land surface model with multiparameterization options (Noah-MP): 1. Model description and evaluation with local-scale measurements. *J Geophys Res* 116, D12109. doi:10.1029/2010JD015139
- Rasmussen R et al (2010) High-resolution coupled climate runoff simulations of seasonal snowfall over Colorado: a process study of current and warmer climate. *J Clim* 24:3015–3048
- Schar C, Luthi D, Beyerle U (1999) The soil-precipitation feedback: a process study with a regional climate model. *J Clim* 12:722–741
- Seuffert G, Gross P, Simmer C (2002) The influence of hydrologic modeling on the predicted local weather: Two-way coupling of a mesoscale weather prediction model and a land surface hydrologic model. *J Hydrometeorol* 3:505–523
- Skamarock WC, Klemp JB, Dudhia J, Gill DO, Barker DM, Duda M, Huang X.-Y, Wang W, Powers JG (2008) A Description of the Advanced Research WRF Version 3, NCAR Technical Note, p 384
- Trier S, Chen F, Manning K, LeMone MA, Davis C (2008) Sensitivity of the simulated PBL and precipitation to land surface conditions for a 12-Day warm-season convection period in the Central United State. *Mon Weather Rev* 136:2321–2343
- Zaitchik B, Santanello J, Kumar S, Peters-Lidard C (2013) Representation of soil moisture feedbacks during drought in NASA Unified WRF. *J Hydrometeorol* 14:360–367
- Zeng X, Barlage M, Castro C, Fling K (2010) Comparison of land–precipitation coupling strength using observations and models. *J Hydrometeorol* 11:979–994